Integrative Biology

Accepted Manuscript

ROYAL SOCIETY OF CHEMISTRY

www.rsc.org/ibiology

The Lateral Diffusion and Fibrinogen Induced Clustering of Platelet Integrin $\alpha_{IIb}\beta_3$ Reconstituted into Physiologically Mimetic GUVs.

Vinnie Gaul,[1] Sergio Lopez,[1] Barry Lentz,[2*] Niamh Moran,[3] Robert R. Forster,[1] Tia E. Keyes[1*]

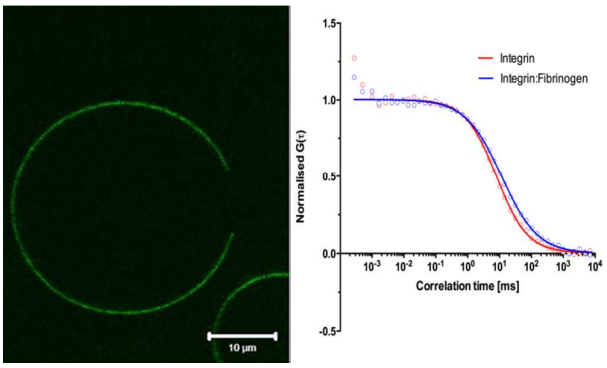

A novel method for reconstitution of Integrin $\alpha_{IIb}\beta_3$ into GUVs with unrestricted lipid composition is described and the lateral diffusion and phase partitioning of the integrin with activation and ligand binding in biomimetic GUVs compositions is described.

The Lateral Diffusion and Fibrinogen Induced Clustering of Platelet Integrin $\alpha_{IIb}\beta_3$ Reconstituted into Physiologically Mimetic GUVs.

Vinnie Gaul,[1] Sergio Lopez,[1] Barry Lentz,[2*] Niamh Moran,[3] Robert J. Forster,[1] Tia E. Keyes[1*]

1. School of Chemical Sciences and National Biophotonics and Imaging Platform, Dublin City University, Dublin 9, Ireland

2. Biophysics Department, University of North Carolina at Chapel Hill, Chapel Hill, North Carolina, USA

3. Molecular and Cellular Therapeutics Department, Royal College of Surgeons Ireland, Dublin 2, Ireland

Abstract

Platelet integrin $\alpha_{IIb}\beta_3$ is a key mediator of platelet activation and thrombosis. Upon activation it undergoes significant conformational rearrangement, inducing complex bidirectional signalling and protein recruitment leading to platelet activation. Reconstituted lipid models of the integrin can enhance our understanding of the structural and mechanistic details of $\alpha_{IIb}\beta_3$ behaviour away from the complexity of the platelet machinery. Here, a novel method of $\alpha_{IIb}\beta_3$ insertion into Giant Unilamellar Vesicles (GUVs) is described that allows for effective integrin reconstitution, unrestricted by lipid composition. $\alpha_{IIb}\beta_3$ was inserted into two GUV lipid compositions that seek to better mimic the platelet membrane. First, "nature's own", comprising 32% DOPC, 25% DOPE, 20% CH, 15% SM and 8% DOPS, intended to mimic the platelet cell membrane. Fluorescence Lifetime Correlation Spectroscopy (FLCS) reveals that exposure of the integrin to the activators Mn^{2+} or DTT does not influence the diffusion coefficient of . Similarly, exposure to $\alpha_{IIb}\beta_3$'s primary ligand fibrinogen (Fg) alone does not affect $\alpha_{IIb}\beta_3$ diffusion coefficient. However, addition of Fg and either activator

reduces the integrin diffusion coefficient from 2.52 ± 0.29 to $\mu m^2.s^{-1}$ to 1.56 ± 0.26 (Mn^{2+}) or 1.49 ± 0.41 $\mu m^2.s^{-1}$ (DTT) which is consistent with aggregation of activated $\alpha_{IIb}\beta_3$ induced by fibrinogen binding. The Multichannel Scaler (MCS) trace shows that the integrin-Fg complex diffuses through the confocal volume in clusters. Using the Saffman-Delbrück model as a first approximation, the diffusion coefficient of the complex suggests at least a 20-fold increase in the radius of membrane bound protein, consistent with integrin clustering. Second, $\alpha_{IIb}\beta_3$ was also reconstituted into a "raft forming" GUV with well defined liquid disordered (L_d) and liquid ordered (L_o) phases. Using confocal microscopy and lipid partitioning dyes, $\alpha_{IIb}\beta_3$ showed an affinity for the DOPC rich L_d phase of the raft forming GUVs, and was effectively excluded from the cholesterol and sphingomyelin rich L_o phase. Activation and Fg binding of the integrin did not alter the distribution of $\alpha_{IIb}\beta_3$ between the lipid phases. This observation suggests partitioning of the activated fibrinogen bound $\alpha_{IIb}\beta_3$ into cholesterol rich domains is not responsible for the integrin clustering observed.

Introduction

$\alpha_{IIb}\beta_3$, also known as GPIIb/IIIa, is a member of the integrin family of cell surface receptor proteins which resides specifically at the surface of the blood platelet where it plays a key role in signalling during thrombosis.[1] Integrins are adhesion receptors found ubiquitously in metazoan cells. They facilitate cell migration and extracellular matrix assembly and are involved in a wide range of activities, including immune response, cell proliferation and apoptosis.[2] Like all 24 members of the integrin family, $\alpha_{IIb}\beta_3$ is a heterodimer of an alpha and beta subunit that spans the platelet plasma membrane once.[3] $\alpha_{IIb}\beta_3$ is the most abundant receptor on the platelet surface, numbering between 50,000 to 80,000 copies per platelet. Its primary ligand is the soluble plasma glycoprotein fibrinogen, which is found en masse in the bloodstream. Fibrinogen consists of an α, β and γ chain, with recognition sequences for platelet integrin $\alpha_{IIb}\beta_3$ within the α and γ chains. The Fibrinogen structure mediates coupling of platelets via their $\alpha_{IIb}\beta_3$ surface proteins, thus promoting platelet aggregation. Other cell adhesion molecules present on the endothelial cell matrix such as vWF, fibronectin, and vitronectin, also have affinity for fibrinogen and facilitate the localisation of a clot to the active endothelium.[4,5,6]

In order to prevent the formation of thrombi under normal physiological conditions, the interaction of platelets with their environment is strictly regulated. For example, the recognition of fibrinogen by $\alpha_{IIb}\beta_3$ is dependent on intracellular proteins that interact with the cytoplasmic domain of the integrin protein. In typical thrombus formation, initial interaction of platelets with the ECM at the site of vascular injury is mediated by glycoprotein (GP) Ib/IX/V complex, collagen receptors, GP VI and integrin $\alpha_2\beta_1$ on the platelet surface, as well as by vWF and fibrillar collagen at the vascular site. Subsequently, soluble agonists such as ADP, which is released from platelet dense granules, or thrombin and TxA2, produced at the site of injury, act to amplify platelet activity as well as recruit additional platelets to the lesion location. These agonists interact with their respective receptors on the platelet surface to initiate an intracellular signalling pathway within the platelet, leading

ultimately to $\alpha_{IIb}\beta_3$ activation via its cytoplasmic tail in a process known as "inside-out signalling".[7] Activation precipitates conformational change of $\alpha_{IIb}\beta_3$ leading to fibrinogen binding, and integrin clustering at the platelet surface which is believed to play a key role in driving signalling and receptor recognition.[8] Upon ligand binding, an additional signal is sent inside the cell, in a process known as "outside-in signalling". Thus, $\alpha_{IIb}\beta_3$ is capable of bidirectional signalling. Outside-in signalling leads to reinforcement of the thrombus via integrin clustering and downstream activation of kinases that stabilize the integrin mediated links between ECM proteins and actin filaments.[9]

In platelet studies, integrin activation and platelet aggregation is commonly promoted by a variety of activators, such as thrombin, ADP, collagen, and thromboxane A_2. These agonists, they do not act directly on the integrin but rather on their respective receptor molecules to induce an intracellular signalling cascade leading to a rise in cytosolic calcium, activation of PKC and PI3K, as well as engagement of talin with $\alpha_{IIb}\beta_3$.[7] In addition to these physiological activators of $\alpha_{IIb}\beta_3$, a number of other non-physiological integrin activators are commonly used to induce integrin activation, such as reducing agent dithiothreitol (DTT) and divalent cation Mn^{2+}.[10] In contrast to the physiological activators, these artificial activators act directly on the integrin molecule itself rather than acting through intracellular pathways. DTT functions to reduce two disulphide bonds within the integrin's cysteine-rich domain, which leads to a structural and allosteric change in $\alpha_{IIb}\beta_3$. This change in conformation is believed to open up the integrin headpiece to permit ligand binding.[11] In contrast to DTT, Mn^{2+} does not appear to bring about the same global conformational changes in the integrin. Conflicting reports exist on the exact structural changes observed in integrin when subjected to Mn^{2+}, with some reports suggesting a "switchblade" like extension of the integrin molecule[12], while others suggest that no extension of the integrin molecule occurs.[13] The differences observed between these two mimics of integrin activation suggest the multiple structural configurations exist in $\alpha_{IIb}\beta_3$, but how close these states are to physiological conformations is a matter for debate.[14]

An important avenue for understanding $\alpha_{IIb}\beta_3$ structure and behaviour within the platelet membrane is to study it reconstituted into artificial membrane models, away from the complexity of its physiological home. A number of elegant studies have explored $\alpha_{IIb}\beta_3$ incorporated into supported lipid bilayers (SLB)[15,16], nanodiscs[17], or lipid vesicles[18]. Reconstitution has been into simple binary or ternary lipid compositions, whereas in reality the cell membrane is composed of thousands of different lipids [19]. While replication of such a complex system is not practical, a composition that features the major components of the cell membrane is desirable, but not thus far achieved for $\alpha_{IIb}\beta_3$. For example, the most common phospholipids of the platelet membrane are phosphatidylcholine, phosphatidylethanolamine, and phosphatidylserine, while the sphingolipid sphingomyelin and the sterol cholesterol are also present in significant quantities (approximately 25 % of the total lipid content).[20] Furthermore, there are relatively few studies on the dynamics of integrin diffusion in artificial systems, and those studies that do exist have focussed on Fluorescence Recovery After Photobleaching (FRAP) in SLBs.[15,16,21] FRAP makes substantial demands in terms of label quantity and is not especially useful alone for unequivocally identifying aggregation. Furthermore, there are relatively few studies of integrin diffusional dynamics in liposomes despite their value in studying proteins with large extracellular or cytoplasmic domains, which can severely hinder protein motion in SLBs and related structures.

Here, we reconstituted $\alpha_{IIb}\beta_3$ in free standing physiologically relevant GUVs and have used Fluorescence Lifetime Correlation Spectroscopy (FLCS) for the first time to study $\alpha_{IIb}\beta_3$ diffusion in these biomimetic liposome formulations. The platelet cell membrane-like lipid composition used was adopted from a formulation designed by Lentz et al.[22] This composition, referred to as “nature’s own”, is composed of 32 % DOPC, 25 % DOPE, 20 % CH, 15 % SM and 8 % DOPS. In addition to this physiologically relevant composition, a cholesterol rich, lipid raft forming composition was also used to identify whether $\alpha_{IIb}\beta_3$ shows preference for liquid disordered or liquid ordered domains. This was composed of 50 % DOPC, 25 % CH and 25 % SM. $\alpha_{IIb}\beta_3$ diffusion and partitioning in these liposomes were compared under different activation and ligand bound states.

Materials and Methods

Materials

1,2-dioleoyl-3-sn-phosphatidylcholine (DOPC), 1,2-dioleoyl-3-sn-phosphatidylethanolamine (DOPE), 1,2-dioleoyl-3-sn-phosphatidylserine (DOPS), bovine brain sphingomyelin (SM), cholesterol (CH) were purchased from Avanti Polar Lipids (Alabama, USA). Integrin $\alpha_{IIb}\beta_3$ was purchased from Enzyme Research Laboratories (Swansea, UK). ATTO 655 N-hydroxysuccinimide (NHS) ester was purchased from ATTO-TEC (Siegen, Germany). Bio-beads were obtained from Life Science (Dublin, Ireland). DiD was purchased from Invitrogen (Dublin, Ireland). TAMRA NHS ester, HEPES, NaCl, $CaCl_2$, Triton X-100 and Sephadex G-25 were acquired from Sigma-Aldrich (Wicklow, Ireland). Purified human fibrinogen was purchased from Merck Millipore (Cork, Ireland). All aqueous solutions were prepared using MilliQ water (Millipore Corp., Bedford, USA).

Integrin Labelling

Atto 655 NHS ester or TAMRA NHS ester was dissolved in DMF at 2 mg/ml, added to a HEPES/triton X100 solution of $\alpha_{IIb}\beta_3$ in fivefold molar excess, and gently stirred for 2 hours at room temperature. Labelled protein was then separated from unbound dye via size exclusion chromatography (Sephadex G-25). The labelling ratio was determined via UV-Vis spectroscopy to be 1:1

Integrin Reconstitution

Lipids, dissolved in chloroform at the desired composition, were dried under a steady stream of nitrogen in a glass vial before being placed under vacuum for 2 hours to ensure solvent evaporation. For lipid diffusion studies DOPE-atto532 was also included at a concentration of 0.001 mol % in the lipid content, while for partitioning studies, the lipophilic tracer dye, DiD was included. The lipid was

then solubilised at 1 mM in a reconstitution buffer (10 mM HEPES, 150 mM NaCl, 1 mM $CaCl_2$, 0.1% Triton X-100, pH 7.4). Labelled $\alpha_{IIb}\beta_3$ was added to the vial before the solution was shaken at room temperature for 30 minutes to ensure that all lipid has been solubilised and that the solution was homogenous. The solution was then incubated at 37 °C for 1.5 hours. The detergent was removed by incubation of the solution with 100 mg of biobeads per ml of solution for 3.5 hours in a slowly shaken vial. Following which time the biobeads were removed and replaced by a fresh batch of 100 mg biobeads per ml of solution and incubated for a further 30 minutes (slowly shaken). Once purification was complete the biobeads were removed and the reconstituted proteo-liposomes were stored at 4°C for later use. The final density of integrin within the liposome was estimated from the average number of fluorescent molecules within the focal volume (N), to be 0.042 protein/μm^2. (Supplementary information)

GUV creation

Proteoliposomes in HEPES buffer were ultracentrifuged at 100,000 g for 1 hour at 4 °C in order to pellet the vesicles. The pellet was then gently washed with deionised H_2O before being re-suspended in deionised H_2O at a lipid concentration of 10 mM. The lipid was then pipetted in 2 µl droplets on the conductive side of an indium tin oxide (ITO) glass slide. To partially dehydrate the lipid droplets, the slide was placed in a vacuum desiccator in the presence of a saturated sodium chloride solution for at least 2 hours. After partial dehydration, the electroformation cell was assembled and filled with electroformation buffer (10 mM HEPES, 150 mM NaCl, 1 mM $CaCl_2$, 100 mM sucrose, pH 7.4). For electroformation, an AC electric field provided by a pulse generator was applied overnight across the chamber and was linearly increased to 1 V over the first hour before being held constant. The frequency was kept at 500 Hz throughout. For observation, GUVs were removed from the electroformation cell and added to an observation buffer (10 mM HEPES, 150 mM NaCl, 1 mM $CaCl_2$, 100 mM glucose, pH 7.4) within an observation chamber. (Representative images of the as-formed GUVs from this protocol are shown in the supplementary information). In order to keep the GUVs

stationary for point measurements, the GUVs were electroformed in a 100 mM sucrose-containing buffer and later transferred to a 100 mM glucose-containing buffer. The difference in density between the inner sucrose buffer and the outer (mostly) glucose buffer allowed for their sedimentation on the glass substrate while keeping osmolality constant. This technique is commonly used to create stationary GUVs.[23–26]

Confocal Microscopy

Confocal images were taken using a MicroTime 200 fluorescence lifetime microscope system (PicoQuant GmbH, Berlin, Germany). Fluorophores were excited with 532-nm PicoTA or 640-nm light from a LDH-P-C-640B diode laser. The laser was directed toward a z532/635rpc dichroic mirror and focused on a water immersion objective (NA 1.2 UPlanSApo 60× 1.2 water/CC1.48, Olympus). The sample fluorescence was collected through the same objective and filtered by the aforementioned dichroic mirror, as well as by an HQ550lp AHF/Chroma filter (Olching, Germany) for the 532-nm laser, or a BLP01-635R-25 Semrock filter (New York, USA) for the 640-nm laser. Finally, the sample fluorescence was passed through a 50-μm pinhole onto a MPD SPAD detector.

Fluorescence Lifetime Correlation Spectroscopy (FLCS)

Diffusion coefficients for labelled integrin or lipid were obtained using fluorescence lifetime correlation spectroscopy, FLCS. The autocorrelation functions obtained using FLCS are less prone to noise and distortion caused by scattered excitation light, detector thermal noise and detector afterpulsing than conventional FCS.[27] FLCS measurements were performed using a MicroTime 200 confocal fluorescence lifetime microscope system. For FLCS experiments, the fluorophores were excited as before and the sample fluorescence was also collected as described for confocal microscopy. The autocorrelation functions (ACF) were fit using SymphoTime software (PicoQuant GmbH, Berlin, Germany), to Equation (1):

$$G(\tau) = \frac{1}{N(1-T)}\left[1 - T + T\,e^{\left(-\frac{\tau}{\tau_T}\right)}\right]\left[1 + \left(\frac{\tau}{\tau_D}\right)^{\alpha}\right]^{-1} \quad (1)$$

where $G(\tau)$ is the autocorrelation function of fluorescence fluctuations; τ is the delay time; N is the number of fluorophores in the effective volume; T is the fraction of the molecules in the triplet state; τ_T is the relaxation time for the singlet-triplet crossing; α is the anomalous parameter; and τ_D is the diffusion time, which is related to the lateral diffusion coefficient (D_L) of the labelled tracer by the expression: $\tau_D = \omega_0^2 / 4D_L$. In the latter equation, the radius ω_0 is the distance at which the excitation intensity profile decreases to e^{-2} of its maximum value. This parameter was determined experimentally as described previously, by measuring the translational diffusion of Rhodamine 6G (532-nm laser) and Atto655 (640-nm laser) in water at room temperature (≈ 21 °C).[28] These dyes, have well characterized diffusion coefficients and so were used as standards to determine the working confocal volume for FLCS measurements.

Before performing FLCS point measurements, confocal images were collected to identify and locate suitable GUVs for study, representative images are shown in Figure 8, supplementary material. In order to avoid the sharp curvature of smaller GUVs or undulations in larger GUVs, only single unilamellar vesicles with diameters within the range 20 and 40 µm were selected for FLCS measurements. This selection criteria was based on that recommended by Ramadurai et al.[29] To precisely locate the lipid bilayer of the liposome where FLCS measurements were to be taken, fluorescence intensity measurements were performed by z-scanning near the GUV membranes until the site of maximum intensity was located. Point FLCS measurements were then recorded at these precise positions for 3 minutes. Throughout the measurement, the MCS trace was monitored to ensure that the GUVs remained stationary during FLCS recording. Recordings from GUVs that exhibited drift during the measurement were eliminated from the analysis.

To obtain statistically significant $\alpha_{IIb}\beta_3$–Atto655 diffusion coefficients, typically between one and three measurements were collected from each GUV. The integrin diffusion coefficients values quoted are based on between 60 and 80 point measurements, meaning that the diffusion value is an average of values taken across between 50 and 60 different GUVs of the dimensions described and the standard deviations quoted are derived from this number of measurements. The lipid diffusion coefficients (Figure 2/Table 1) are based on 39 point measurements of between 120 and 180 seconds across 30 different GUVs.

Results

Lipid and integrin diffusion in "nature's own" GUVs

FLCS measurements were performed by monitoring the autocorrelation functions separately each of the labelled lipid (DOPE-Atto532) and labelled protein ($\alpha_{IIb}\beta_3$–Atto655) in order to determine their respective diffusion coefficients in GUVs composed of the nature's own composition. A typical autocorrelation function and its fit to a single component, two dimensional diffusion model (equation (1)) is shown in **Figure 1**. The diffusion co-efficient of DOPE-Atto532 within the "nature's own" bilayer was found to be 7.89 ± 0.42 $\mu m^2/s$ at room temperature, with an α value of 1.01 ± 0.04, i.e., the mean-squared displacements of the lipid scale as a power law of time with an exponent α of 1 indicating that the lipid is undergoing normal Brownian diffusion at the liposome interface. α values of greater or less than one, indicate anomalous diffusion, which in the case of a value less than 1 is usually attributed to hindered diffusion due to barriers within the membrane.[30] The lipid diffusion value is consistent with values reported previously for GUVs comprised of ternary lipid mixtures as determined by FCS.[31,32]

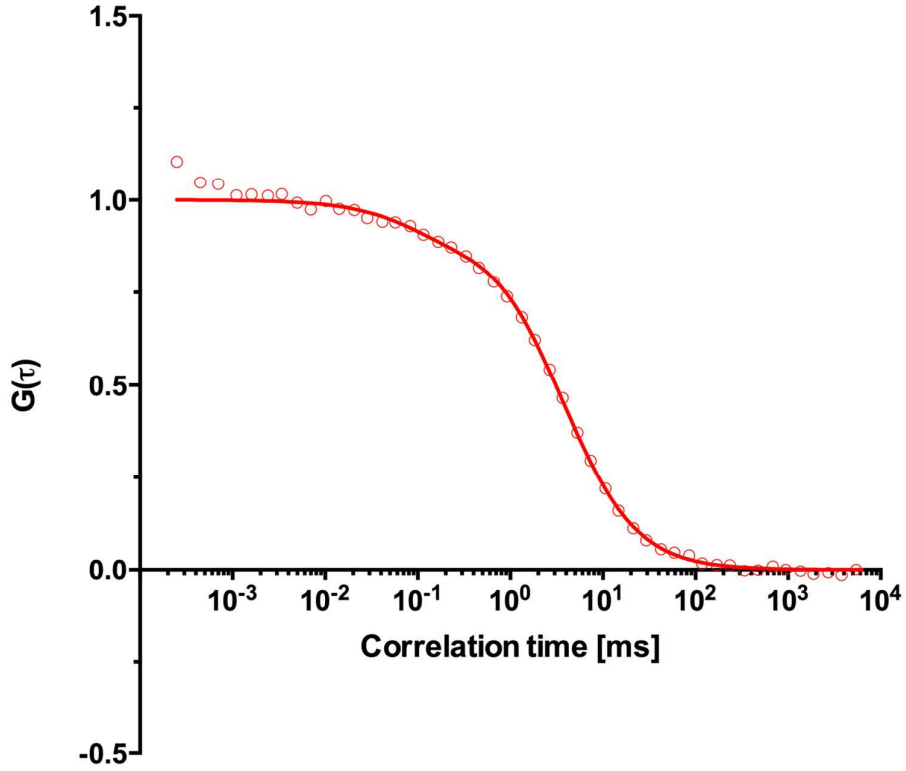

Figure 1: A typical autocorrelation function and its single component two dimensional fit (equation 1) for DOPE-atto532 diffusing in nature's own GUVs at room temperature. GUVs created via the electroformation protocol in a sucrose containing buffer were pipetted into an observation buffer of 10 mM HEPES, 150 mM NaCl, 1 mM $CaCl_2$, 100 mM glucose, pH 7.4, and the GUVs were allowed to come to rest on the bottom of a glass slide over a 30 minute period. Stationary GUVs were selected before a point measurement was performed on the GUV membrane. DOPE-atto532 diffusion in nature's own GUVs was determined to be 7.89 ± 0.42 $\mu m^2/s$ at room temperature.

A typical autocorrelation function and its fit to a single component two dimensional model (equation 1) for $\alpha_{IIb}\beta_3$-atto655 in a "nature's own" GUV is shown in Figure 2 (red curve). The diffusion co-efficient was determined to be 2.52 ± 0.29 $\mu m^2/s$ at room temperature in GUVs. An α value of approximately 1 (0.99 ± 0.03) was obtained indicating that resting integrin in nature's own composition is diffusing normally. The ACF fits well to a single component model with no evidence for slower diffusing components, associated, for instance, with aggregated protein. In order to detect whether $\alpha_{IIb}\beta_3$ was already in its ligand binding conformation prior to activator addition, fibrinogen was pipetted into the observation chamber to a final concentration of 0.1 mg/ml, incubated for 1 hour, and the diffusion co-efficient of the $\alpha_{IIb}\beta_3$-Atto655 was again measured. The

diffusion co-efficient, 2.61 ± 0.35 $\mu m^2/s$, and α values, 0.99 ± 0.02, are indistinguishable from those observed prior to incubation with fibrinogen, indicating that, as expected, the $\alpha_{IIb}\beta_3$ remained unbound to its ligand, Fg. Thus, $\alpha_{IIb}\beta_3$ as reconstituted into the "nature's own" GUVs appears to remain in its native, resting conformation. This is further confirmed vide infra, where a significant change in the diffusion coefficient is induced by fibrinogen binding following its chemical activation with either DTT or Mn^{2+}.

$\alpha_{IIb}\beta_3$ diffusion after activation and ligand binding

To investigate whether the conformational changes induced by nominally activating $\alpha_{IIb}\beta_3$ resulted in a measureable change to its diffusion co-efficient determined by FLCS, activators DTT or Mn^{2+} were applied to the integrin. To do this, DTT or Mn^{2+} solution was carefully pipetted into the observation chamber containing the $\alpha_{IIb}\beta_3$ reconstituted GUVs to a final activator concentration of 3 mM The integrin and activator were incubated at room temperature for 1 hour before FLCS measurement commenced. Following incubation with DTT, the diffusion co-efficient of liposome-bound $\alpha_{IIb}\beta_3$ was determined by FLCS to be 2.59 ± 0.24 $\mu m^2/s$, whilst for liposome-bound $\alpha_{IIb}\beta_3$ incubated with Mn^{2+}, a diffusion co-efficient of 2.51 ± 0.19 $\mu m^2/s$ was obtained. In both cases, the α values were found to be approximately 1. Together these results indicate that the conformational (hydrodynamic volume) changes induced in $\alpha_{IIb}\beta_3$ by DTT or Mn^{2+} are not alone sufficient to induce a measureable change in integrin diffusion coefficient. Furthermore, the ACFs fit well to a single component model with no evidence for slower diffusing components in the ACF which might suggest integrin clustering.

On the basis of the unchanging diffusion coefficients, fibrinogen does not bind to the resting $\alpha_{IIb}\beta_3$ reconstituted into nature's own liposome. However when the $\alpha_{IIb}\beta_3$–liposome assembly was incubated with 3mM DTT or 3 mM Mn^{2+} *and* fibrinogen (0.1 mg/ml), a significant change in the diffusion co-efficient was observed. The co-addition of DTT and fibrinogen reduced the diffusion coefficient to 1.56 ± 0.26 $\mu m^2/s$. Similarly, co-addition of Mn^{2+} and fibrinogen to $\alpha_{IIb}\beta_3$ reconstituted

into liposome resulted in a diffusion co-efficient of 1.49 ± 0.41 $\mu m^2/s$. These results suggest that the DTT or manganese activated integrin binds fibrinogen and the resulting complex diffuses more slowly.

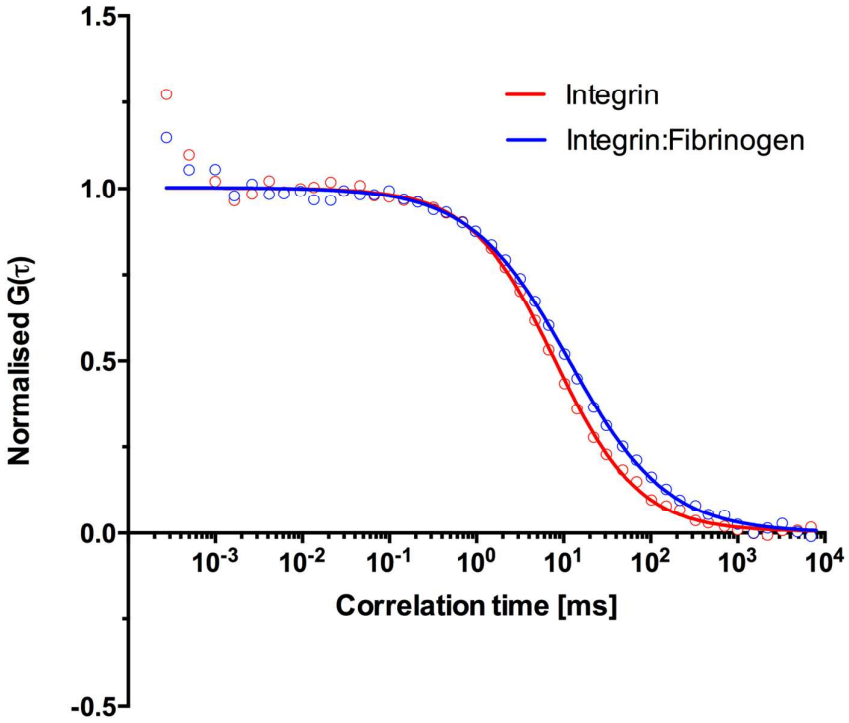

Figure 2: Representative single component fits (solid lines) to ACFs collected from resting $\alpha_{IIb}\beta_3$–atto655 (red) and activated, fibrinogen bound $\alpha_{IIb}\beta_3$–Atto655 (blue) in nature's own GUVs at room temperature. The $\alpha_{IIb}\beta_3$ reconstituted GUVs were created in a sucrose containing buffer before being pipetted into an observation buffer of 10 mM HEPES, 150 mM NaCl, 1 mM $CaCl_2$, 100 mM glucose at pH 7.4. The GUVs were allowed to come to rest on a glass slide over a 30 minute period prior to measurement. Stationary GUVs were selected before a point measurement was performed on the GUV membrane. $\alpha_{IIb}\beta_3$-Atto655 diffusion in nature's own GUVs before the addition of activators or fibrinogen was determined to be 2.52 ± 0.29 $\mu m^2/s$ at room temperature. Following integrin activation and addition of fibrinogen, this diffusion co-efficient reduced to 1.56 ± 0.26 $\mu m^2/s$ with DTT and 1.49 ± 0.41 $\mu m^2/s$ with Mn^{2+}.

The Saffman-Delbrück model,[33] is one of the most widely used models used to describe the 2 dimensional diffusion of protein bound to a membrane. According to this description, the diffusion co-efficient of a membrane protein integrated into a lipid membrane exhibits logarithmic dependence on the reciprocal of the hydrodynamic radius R, of the protein as expressed by equation 2:[29]

$$D = \frac{k_B T}{4\pi\mu_m h}\left(\ln\left(\frac{\mu_m h}{\mu_w R}\right) - 0.5772\right) \quad (2)$$

Where *D* is the lateral diffusion co-efficient of the protein, k_B is Boltzmann constant, T is the absolute temperature, *h* is the thickness of the lipid bilayer, μ_m is the viscosity of the lipid bilayer and μ_w is the viscosity of the surrounding aqueous phase. Although there have been challenges to the broad veracity of the SD model,[34] there are numerous convincing studies which demonstrate its applicability across membrane proteins with hydrodynamic radii up to approximately 10 nm.[29,35] The integrin within both resting and activated conformational ranges have hydrodynamic radii below this value.[36] According to the SD model, the only parameter of the protein exerting an influence on its diffusion coefficient is its hydrodynamic radius and this value weakly affects the diffusion co-efficient. For example, increasing the protein radius from 1 nm to 10 nm only changes the mobility by 30 %.[34] Here, upon fibrinogen binding, the diffusion coefficient of $\alpha_{IIb}\beta_3$ decreases by approximately 40 % when compared with unbound, resting $\alpha_{IIb}\beta_3$. This suggests, relying on the Saffman-Delbrück model as a first approximation, a 20-fold increase in the radius of the diffusing protein following ligand binding.* Such an increase is too large to be accounted for by the formation of 1:1 or even 1:2 Fg-$\alpha_{IIb}\beta_3$ complexes. Rather, it strongly suggests that significant aggregation of the

* As the Safman-Delbrück model is limited to proteins with hydrodynamic radii below 10 nm, it is likely the estimate of the cluster size is an underestimate, as studies have shown that for hydrodynamic radii exceeding 10 nm a 1/R dependency applies.[31]

integrin is occurring on Fg binding following $\alpha_{IIb}\beta_3$ activation by either DTT or Mn^{2+}. In turn, fibrinogen binding and aggregation only occur after treatment of the integrin with the activator. Furthermore, importantly, as shown in Table 1, the integrin diffusion coefficient is anomalous following Fg binding, reflected in a significant deviation of α from unity. An α of 0.87 ± 0.03 was obtained for integrin treated with DTT + fibrinogen and 0.88 ± 0.03 for integrin treated with Mn^{2+} + fibrinogen. Consistent with the formation of aggregates that act as barriers in the bilayer,[30] these values suggest that protein lateral diffusion is hindered.

Table 1: Lipid and integrin $\alpha_{IIb}\beta_3$ diffusion in nature's own GUVs. The table shows the diffusion coefficient before activation in the presence and absence of fibrinogen, and after activation in the presence and absence of fibrinogen. Activation or ligand addition alone was not sufficient to bring about a measurable change in $\alpha_{IIb}\beta_3$ diffusion. The combination of activation and ligand addition was sufficient to bring about a reduction in diffusion of $\alpha_{IIb}\beta_3$ attributed to integrin aggregation. Furthermore, the combination of activation and ligand addition led to anomalous diffusion of $\alpha_{IIb}\beta_3$ as indicated by the alpha values.

Conditions	Diffusion co-efficient ($\mu m^2/s$)	α
Lipid (DOPE-atto532)	7.89 ± 0.42	1.01 ± 0.04
$\alpha_{IIb}\beta_3$	2.52 ± 0.29	0.99 ± 0.03
$\alpha_{IIb}\beta_3$ + fibrinogen	2.61 ± 0.35	0.99 ± 0.02
$\alpha_{IIb}\beta_3$ + 3mM DTT	2.59 ± 0.24	1.02 ± 0.03
$\alpha_{IIb}\beta_3$ + 3mM Mn^{2+}	2.51 ± 0.19	1.02 ± 0.04
$\alpha_{IIb}\beta_3$ + 3mM DTT + fibrinogen	1.56 ± 0.26	0.87 ± 0.03
$\alpha_{IIb}\beta_3$ + 3mM Mn^{2+} + fibrinogen	1.49 ± 0.41	0.88 ± 0.03

To further examine the possibility of the formation of integrin aggregates, the Multichannel Scaler (MCS), or fluorescence time traces from single point measurements taken in the plane of the lipid bilayer membrane were examined. The MCS trace allows us to compare the fluorescence fluctuations over time within the focal volume. Each fluorescent burst in the MCS corresponds to the transit of a single fluorescently labelled integrin through the detection volume. Typical MCS

traces for $\alpha_{IIb}\beta_3$ and activated $\alpha_{IIb}\beta_3$ in the presence of fibrinogen are shown below in **Figure 3** (top and bottom respectively).

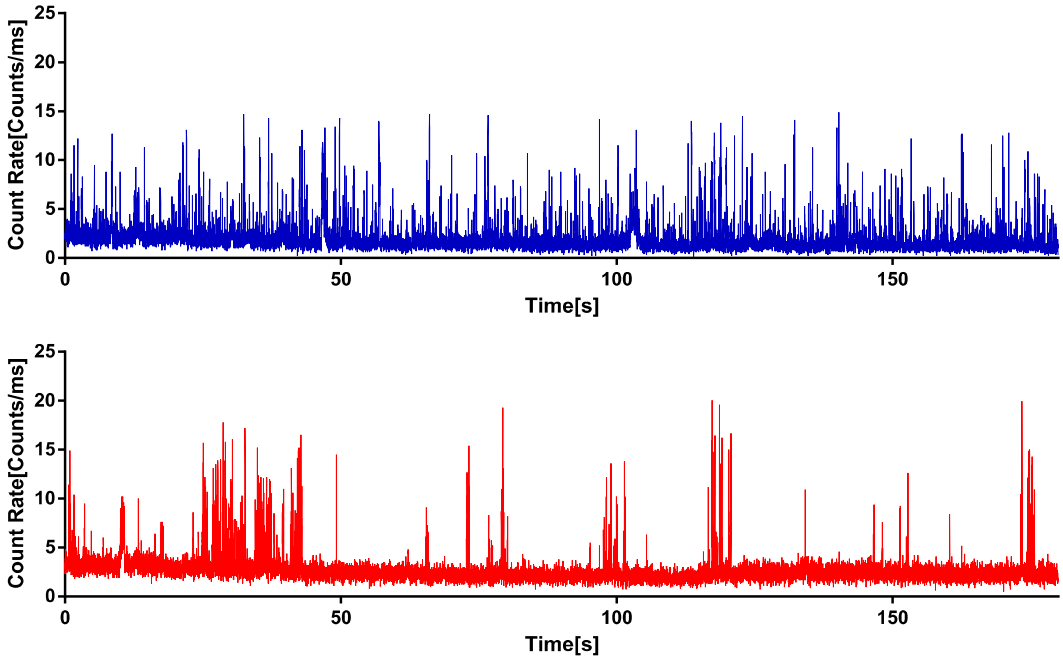

Figure 3: Fluctuating photon-counting time traces, binned at 1-ms resolution, from single point measurements in the plane of the liposome membrane. The upper trace (blue) shows diffusion of un-activated Tamra labelled-$\alpha_{IIb}\beta_3$ in nature's own GUVs while the lower trace (red) shows diffusion of DTT activated Tamra labelled-$\alpha_{IIb}\beta_3$ in nature's own GUVs following the addition of fibrinogen. The un-activated form of $\alpha_{IIb}\beta_3$ passes through the focal volume with a regular fairly homogeneous frequency. Whereas, Fibrinogen bound $\alpha_{IIb}\beta_3$ passes through the focal volume in heterogeneous, irregular bursts, each burst appears to contain clusters of fluorophores migrating together through the focal volume.

Un-activated atto655 labelled $\alpha_{IIb}\beta_3$ diffuses through the focal volume regularly with randomly distributed fluorescence bursts during point measurement. Addition of DTT or Mn^{2+} did not alter the pattern of the MCS trace, nor did Fg alone. However, the addition of fibrinogen to either DTT or Mn^{2+} treated $\alpha_{IIb}\beta_3$ dramatically altered the MCS trace during point measurements. The regular, high frequency of bursts in fluorescence intensity was replaced with less frequent, clustered bursts in the MCS trace. This indicates that groups of the labelled proteins are diffusing together through the confocal volume and is good evidence that integrin is clustering within the bilayer upon fibrinogen binding. (**Figure 3**) It is important to note that the sum of fluorescent intensity before and after

activation and on fibrinogen addition does not change, so although the integrin proteins diffuse through the focal volume in clusters, the total integrin number remains unchanged.

$\alpha_{IIb}\beta_3$ partitions into the liquid disordered phase of cholesterol and sphingomyelin rich GUVs

In order to explore the possibility that clustering of the integrin and its sub-diffusion on activation and ligand binding is precipitated by its segregation into cholesterol/SM rich domains within "nature's own" liposomes, we used the same reconstitution protocol to integrate the labelled $\alpha_{IIb}\beta_3$ into domain forming GUVs. Microdomain forming GUVs were used as due to their sub-wavelength dimensions, lipid rafts are difficult, if not impossible to identify via confocal microscopy. We therefore used GUVs rich in both in cholesterol and sphingomyelin to create domains large enough to view by microscopy. [37] [38] This technique has previously been used to investigate the preferential partitioning of other membrane proteins into lipid domains. For example, syntaxin, synaptobrevin and bacteriorhodopsin have been shown to associate with the liquid disordered phase[39,40], while the GPI-anchored human prion protein, involved in Creutzfeld–Jakob disease associates with the liquid ordered phase.[37]

Whereas $\alpha_{IIb}\beta_3$ has been shown in platelets to exhibit low affinity for detergent resistant (cholesterol rich domains)[41], other integrins have been shown in both artificial membrane models and in cells, to exhibit variable affinity for cholesterol rich domains depending on their activation and ligand binding status.[42,43] Study of phase partitioning of $\alpha_{IIb}\beta_3$ in an artificial membrane system has not been reported to date, presumably because of the limitations of previous reconstitution methods for this protein.

Phase specific fluorescent probes were used to enable facile observation of micron-sized domains in the GUVs using confocal microscopy. To identify the DOPC enriched phase of raft forming GUVs

(50% DOPC, 25 % CH, 25 % SM), the lipophilic tracer dye DiD was used. DiD is a NIR emitting probe with strong affinity for cholesterol poor $l_{d,}$ domains, which is selectively excluded from lipid rafts.[44] Therefore, the co-inclusion of both DiD (abs λ_{max} = 644 nm) and TAMRA labelled integrin (abs λ_{max} = 541 nm) into a domain-forming GUV permitted determination of $\alpha_{IIb}\beta_3$ location with respect to the l_d phase of the liposome.

Figure 4 shows confocal fluorescence images of DiD labelled giant proteoliposomes prepared by the electroformation method, described vide supra. Interestingly, comparison of the fluorescence signal from the separate emission channels for DiD and integrin-TAMRA show very clearly that the two probes co-localize. This suggests that resting $\alpha_{IIb}\beta_3$ exhibits selective affinity for the liquid disordered, DOPC-rich phase, of the phase separated GUVs. This observation is consistent with previous reports on $\alpha_{IIb}\beta_3$ in platelets[41] and with a recent report by Naumann et al on polymer tethered lipid bilayers of ternary lipid mixtures where they observed that the integrins; αvβ3 and α5β1, also sequestered into L_d (cholesterol poor) domains.[42] Naumann et al observed that exposing these integrins to their native ligands; vitronectin or fibronectin, led to integrin sequestering to liquid ordered (L_o) phase domains or loss of specific sequestering respectively for each integrin. We were interested to see if molecular activation and fibrinogen binding of $\alpha_{IIb}\beta_3$ induced similar changes in its domain preference. In an analogous experiment to the FLCS experiment described above, the integrin activators DTT and Mn^{2+} (both at 3 mM) were incubated with $\alpha_{IIb}\beta_3$ reconstituted into raft forming GUVs in the absence of fibrinogen. Confocal fluorescence microscopy showed this did not change the partitioning of $\alpha_{IIb}\beta_3$ in the liposome. The integrin remained sequestered into the L_d regions along with DiD. Interestingly, the addition of integrin activators DTT and Mn^{2+} to $\alpha_{IIb}\beta_3$ in the presence of fibrinogen (0.1 mg/ml), similarly failed to alter its preference for the L_d phase. (Supplementary information) Therefore, in contrast to Naumann et al's observation on integrins $\alpha_v\beta_3$ and $\alpha_5\beta_1$, $\alpha_{IIb}\beta_3$ does not change its affinity for the L_d phase following either activation or ligand binding in a model membrane.[42] Also of note was the apparent tendency of $\alpha_{IIb}\beta_3$ reconstituted GUVs to cluster together following ligand and activator addition. (Supplementary information) This

was observed via confocal microscopy in concentrated GUV solutions. This liposome bunching was not seen in FLCS experiments where GUV solutions were more dilute in order to avoid fluorescence from adjacent GUVs, but is useful evidence that the integrin was activated and ligand bound.

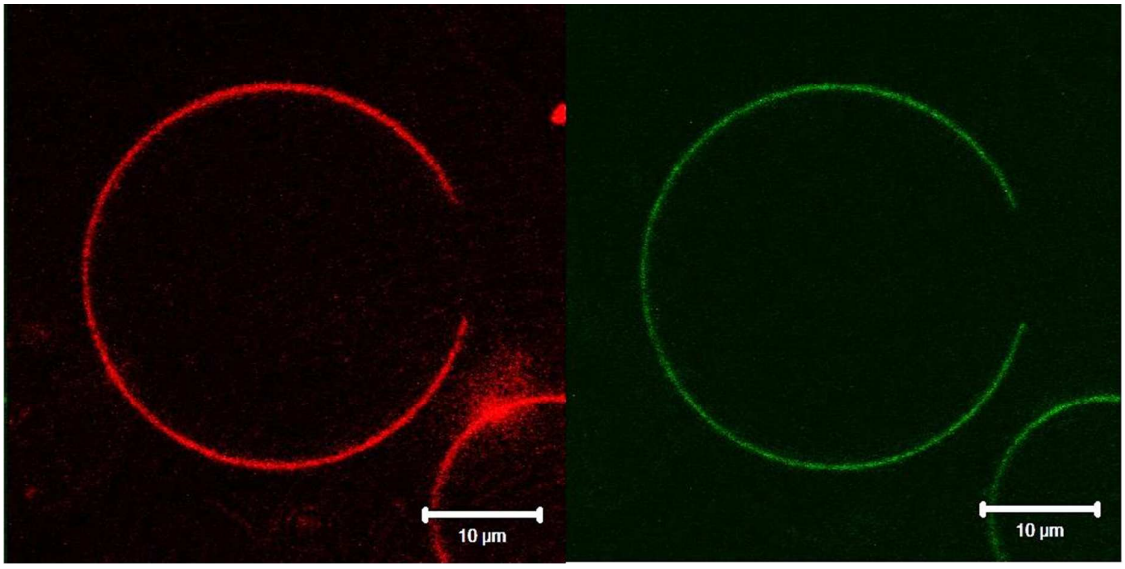

Figure 4: Left) The liquid disordered probe DiD partitioning into the DOPC rich phase of raft forming GUVs composed of 50 % DOPC, 25 % CH and 25 % SM. Right) TAMRA labelled $\alpha_{IIb}\beta_3$ co-localises into the same regions as DiD showing that $\alpha_{IIb}\beta_3$ also has affinity for the liquid disordered phase in raft forming GUVs.

Discussion

According to the method described by Erb and Engel, lipids DMPC or DMPG were required to achieve proper $\alpha_{IIb}\beta_3$ insertion into liposomes, whereas other lipid compositions resulted in loosely bound improperly inserted integrin.[21] Consequently, DMPC and DMPG have been widely used across the literature in artificial membrane systems incorporating integrin $\alpha_{IIb}\beta_3$.[15,16,21,45,46] However, the biological relevance of DMPC lipid is limited, owing particularly to the low levels of 14:0 fatty acid-containing phospholipids in biological systems.[47] Our objective was to reconstitute platelet integrin into a more complex and physiologically relevant lipid composition, to enable study of its diffusion and clustering and to explore sequestering of the integrin in a ternary GUV with domains that were accessible to interrogation by microscopy. The alternative reconstitution process described here

uses a combination of ultracentrifugation and electroformation to create GUVS that only retain properly inserted $\alpha_{IIb}\beta_3$. Failure to carry out the ultracentrifugation and electroformation steps led to loosely bound, or weakly membrane associated $\alpha_{IIb}\beta_3$. It was clear when this occurred as such poorly incorporated integrin showed diffusion co-efficients in excess of the lipid diffusion coefficient. Furthermore, the relative magnitude of the diffusion coefficients reported here for $\alpha_{IIb}\beta_3$ and its surrounding lipid membrane are in good agreement with previous reports on integrin properly incorporated into DMPC/DMPG membranes obtained from FRAP experiments, confirming the integrin was effectively reconstituted.[15,16]

Of particular note, is the fact that the starting $\alpha_{IIb}\beta_3$ concentration had little effect on the final $\alpha_{IIb}\beta_3$ concentration within the GUVs. (Supplementary information) Varying the concentration of protein in the liposome preparation medium led to similar final numbers of $\alpha_{IIb}\beta_3$ diffusing through the focal volume in FLCS measurements, from which we obtain an integrin density of 0.042 integrin/μm^2. Furthermore, there is no evidence for faster diffusing components for $\alpha_{IIb}\beta_3$ in liposomes following ultracentrifugation and electroformation indicating that improperly inserted $\alpha_{IIb}\beta_3$ is efficiently removed.

Previous studies on $\alpha_{IIb}\beta_3$ diffusion have been carried out on SLB systems exploiting FRAP.[15,16,21] An important disadvantage of SLBs applied is that non-specific interactions that can occur between the underlying substrate and the protein extracellular or cytoplasmic domains due to inadequate space (a 10 – 20 Å thick water layer) between substrate and lower bilayer leaflet. Depending on the size of the protein domains, this leads to dramatically slower protein diffusion at SLBs compared to liposome or cell, to partial or complete protein immobilisation or even protein denaturation.[48] The use of GUVs resolves this problem. For our diffusion measurements FLCS was used, because in contrast to FRAP which is destructive and has observation volume in the order of several μm^3, FLCS monitors only femtoliter volumes non-destructively, and is useful in particular, for observing phenomena such as clustering. [27]

In the "nature's own" GUV, a lipid diffusion co-efficient of 7.89 ± 0.42 $\mu m^2/s$ was recorded for labelled DOPE. This value is in agreement with lipid diffusion coefficients recorded in other GUV systems,[49] and is more than twice the value of lipid diffusion in most SLB systems.[15,16,50] Correspondingly, the $\alpha_{IIb}\beta_3$ diffusion coefficient (2.52 ± 0.29 $\mu m^2/s$) in GUV is also significantly higher than reported in SLB systems. Furthermore, as expected, there was no evidence for an immobile fraction. For example, using FRAP on a lipid bilayer formed on quartz slides, Erb *et al* observed a diffusion co-efficient of 0.70 ± 0.06 $\mu m^2/s$ for $\alpha_{IIb}\beta_3$, and 0.58 ± 0.06 $\mu m^2/s$ for fibrinogen bound $\alpha_{IIb}\beta_3$.[15] Goennenwein *et al* observed also using FRAP recorded a diffusion co-efficient of 0.60 ± 0.20 $\mu m^2/s$ for $\alpha_{IIb}\beta_3$ on a cellulose cushioned lipid bilayer.[16] The mobile fraction of integrin in such systems has typically between reported as between 10 and 60 %. The diffusion coefficients we report for $\alpha_{IIb}\beta_3$ are comparable to those reported for whole cells from single particle tracking.[51]

Changes to the $\alpha_{IIb}\beta_3$ diffusion coefficient were only observed when the integrin had been *both* chemically activated *and* exposed to fibrinogen. Fibrinogen treatment of the as-prepared integrin reconstituted liposomes, in absence of activator, had no measureable effect on $\alpha_{IIb}\beta_3$ diffusion coefficient. This was useful confirmation that the reconstitution method we used maintained $\alpha_{IIb}\beta_3$ in its resting state. The magnitude of the reduction in fibrinogen bound $\alpha_{IIb}\beta_3$ diffusion was greater than anticipated for a 1:1 or even 2:1 Fg: $\alpha_{IIb}\beta_3$ complex. Invoking the Saffman-Delbrück model, this indicated the radius of the integrin has increased by a factor of 20 following activation and fibrinogen exposure.[29] The most likely origin of such a large change in hydrodynamic radius is the formation of $\alpha_{IIb}\beta_3$ clusters induced by ligand binding to the activated integrin.[2,52] The MCS trace from point measurements at the liposome interface concurred with this conclusion. Clustering is also consistent with the α value of approximately 0.88 for the activated and ligand bound integrin. This contrasted with the α values of 1 for un-liganded integrin, indicating that free Brownian diffusion switches to hindered sub-diffusion when the integrin is activated and fibrinogen bound, presumably due to barriers formed by the integrin clusters within the bilayer.

In order to investigate if the clustering of the integrin:fibrinogen complex is associated with its partitioning into cholesterol rich rafts, $\alpha_{IIb}\beta_3$ was reconstituted into sphingomylelin and cholesterol rich, phase separated GUVs.

To our knowledge the partitioning of the platelet integrin, $\alpha_{IIb}\beta_3$, has not been studied in an artificial raft forming lipid compositions previously. The relationship of integrin in lipid rafts remains somewhat controversial, whereas $\alpha_{IIb}\beta_3$ has been shown to exhibit low affinity in vivo for the detergent-insoluble fractions of unactivated platelets[53] it has been shown, for example, to participate in the organization of membrane-cytoskeleton interactions at raft domains[54] and as described above, other integrins show clear receptor-ligand binding dependent partitioning in L_o and L_d domains in liposomes.[42,55] Using the ultracentrifugation and electroformation method, $\alpha_{IIb}\beta_3$ was inserted into ternary, cholesterol rich, domain forming liposomes. It was found that resting $\alpha_{IIb}\beta_3$ partitions into the DOPC rich, liquid disordered phase and was excluded from the cholesterol rich domains. Treatment of $\alpha_{IIb}\beta_3$ with integrin activators; DTT and Mn^{2+}, did not alter this liquid disordered phase association. (Supplementary information) This is particularly interesting as physiologically it is believed that activated platelets form lipid rafts, and it is thought that these rafts act as foci that integrate adhesion and signalling molecules.[56] Indeed, parallel studies in leucocytes have shown that integrin activation leads to lipid raft association, thus implicating lipid rafts in the cell adhesion process.[43] As described, $\alpha_V\beta_3$ has been shown to alter preference from L_d domains to L_o domains following ligand binding in artificial lipid models. However, we found that unlike $\alpha_V\beta_3$, $\alpha_{IIb}\beta_3$ did not alter its association with the L_o region either when activated and fibrinogen bound. (Supplementary information) This indicates that the clustering of the integrin in the nature's own composition is not likely to be due to co-clustering of activated fibrinogen bound integrin into cholesterol rich domains.

Conclusions

Using a combination of detergent mediated reconstitution and ultracentrifugation it was demonstrated that it is possible to reproducibly reconstitute platelet integrin $\alpha_{IIb}\beta_3$ into GUVs of varying and complex lipid composition. Using this method, $\alpha_{IIb}\beta_3$ was incorporated into a physiologically relevant lipid composition dubbed "nature's own" comprising 32 % DOPC, 25 % DOPE, 20 % CH, 15 % SM and 8 % DOPS. Using FLCS a diffusion coefficient of 2.52 ± 0.29 to $\mu m^2.s^{-1}$ was measured for the integrin in "Natures Own" GUV. The $\alpha_{IIb}\beta_3$ diffusion values strongly agree with those reported for other integrins in cell membranes, thus confirming the integrin had properly reconstituted into this composition.

Treatment of GUV reconstituted $\alpha_{IIb}\beta_3$ with either DTT or Mn^{2+} did not measurably alter the diffusion coefficient of the integrin. However, addition of fibrinogen to $\alpha_{IIb}\beta_3$ activated with either of these agents, reducing the diffusion coefficient of labelled $\alpha_{IIb}\beta_3$ by approximately 40 % compared with both resting, and activated but un-liganded integrin. In addition, the diffusion behaviour of $\alpha_{IIb}\beta_3$ switched to non-Brownian behaviour, reflected in a decrease in α values from approximately 1 to 0.88 upon ligand binding to the activated integrin. Examination of the MCS or fluorescence time trace showed that fibrinogen binding to the activated form of $\alpha_{IIb}\beta_3$ led to clustering of the fluorescence bursts, attributed to transit of integrin as aggregates through the focal volume. This pattern of diffusion contrasts with the random diffusion pattern of single fluorescently labelled $\alpha_{IIb}\beta_3$. (activated or unactivated) (Figure 3) when not fibrinogen bound. In contrast, addition of fibrinogen to un-activated $\alpha_{IIb}\beta_3$ did not affect its diffusion behaviour, indicating it did not bind in the absence of either DTT or Mn^{2+}.

Combined, these results indicate that both ligand binding and integrin activation are necessary for $\alpha_{IIb}\beta_3$ clustering and that $\alpha_{IIb}\beta_3$ remains in its un-activated form following its reconstitution using the versatile method described here. Analogous studies of $\alpha_{IIb}\beta_3$ reconstituted into ternary, phase separated GUVs co-stained with phase sensitive dyes demonstrated that resting integrin partitions

into the L_d domains of such liposomes. Neither activation of the integrin, with DTT or Mn^{2+}, nor its ligand binding after activation alter the domain preference of $\alpha_{IIb}\beta_3$ which remains sequestered in the L_d phase. This is consistent with platelet studies of $\alpha_{IIb}\beta_3$ which have shown that it does not have strong affinity for cholesterol domains in vivo but contrasts with the behaviour of other integrins such $\alpha_v\beta_3$ and $\alpha_5\beta_1$, which showed varying degrees of mobilisation to the L_o phase upon ligand binding.[42] This result also confirms that the clustering of integrin on activation and ligand binding is not attributed to raft association in the Natures Own GUV.

Overall, this study demonstrates a novel and relatively facile method for reconstitution of platelet integrin, $\alpha_{IIb}\beta_3$ into GUVs of wide and complex lipid composition. This method should facilitate future evaluation of $\alpha_{IIb}\beta_3$ and its ligand interactions away from the complexity of the cell/platelet and will open the possibility of gaining greater understanding of the role of lipid in integrin behaviour.

Acknowledgments

This material is based upon work supported by the Science Foundation Ireland under Grant No. [10/IN.1/B3025] and the National Biophotonics and Imaging Platform, Ireland, and funded by the Irish Government's Programme for Research in Third Level Institutions, Cycle 4, Ireland's EU Structural Funds Programmes 2007 - 2013.

References

1. J. M. Gibbins, *J. Cell Sci.*, 2004, **117**, 3415–25.
2. N. J. Anthis and I. D. Campbell, *Trends Biochem. Sci.*, 2011, **36**, 191–198.
3. M. A. Arnaout, B. Mahalingam and J.-P. Xiong, *Annu. Rev. Cell Dev. Biol.*, 2005, **21**, 381–410.
4. R. R. Hantgan, M. C. Stahle, J. H. Connor, D. A. Horita, M. Rocco, M. A. McLane, S. Yakovlev and L. Medved, *Protein Sci.*, 2006, **15**, 1893–906.
5. J. Sánchez-Cortés and M. Mrksich, *Chem. Biol.*, 2009, **16**, 990–1000.
6. P. Nguyen-Ho and N. M. Lakkis, *Curr. Atheroscler. Rep.*, 2001, **3**, 139–48.
7. J. Rivera, M. L. Lozano, L. Navarro-Núñez and V. Vicente, *Haematologica*, 2009, **94**, 700–711.
8. T. Hato, N. Pampori and S. Shattil, *J. Cell Biol.*, 1998, **141**, 1685–1695.
9. R. R. Hantgan, D. S. Lyles, T. C. Mallett, M. Rocco, C. Nagaswami and J. W. Weisel, *J. Biol. Chem.*, 2003, **278**, 3417–26.
10. R. Litvinov, C. Nagaswami, G. Vilaire, H. Shuman, J. S. Bennett and J. W. Weisel, …, 2004, **104**, 3979–3985.
11. B. Yan and J. W. Smith, *Biochemistry*, 2001, **40**, 8861–8867.
12. J. Takagi, B. M. Petre, T. Walz and T. a Springer, *Cell*, 2002, **110**, 599–11.
13. F. Ye, J. Liu, H. Winkler and K. A. Taylor, *J. Mol. Biol.*, 2008, **378**, 976–86.
14. J. S. Bennett, B. W. Berger and P. C. Billings, *J. Thromb. Haemost.*, 2009, **7 Suppl 1**, 200–5.
15. E. M. Erb, K. Tangemann, B. Bohrmann, B. Müller and J. Engel, *Biochemistry*, 1997, **36**, 7395–402.
16. S. Goennenwein, M. Tanaka, B. Hu, L. Moroder and E. Sackmann, *Biophys. J.*, 2003, **85**, 646–55.
17. F. Ye, G. Hu, D. Taylor, B. Ratnikov, A. a Bobkov, M. a McLean, S. G. Sligar, K. a Taylor and M. H. Ginsberg, *J. Cell Biol.*, 2010, **188**, 157–73.
18. P. Streicher, P. Nassoy, M. Bärmann, A. Dif, V. Marchi-Artzner, F. Brochard-Wyart, J. Spatz and P. Bassereau, *Biochim. Biophys. Acta - Biomembr.*, 2009, **1788**, 2291–2300.
19. G. van Meer and A. I. P. M. de Kroon, *J. Cell Sci.*, 2011, **124**, 5–8.
20. J. S. Owen, R. a Hutton, R. C. Day, K. R. Bruckdorfer and N. McIntyre, *J. Lipid Res.*, 1981, **22**, 423–30.

21. E. M. Erb and J. Engel, *Methods Mol. Biol.*, 2000, **139**, 71–82.

22. S. M. Dennison, M. E. Bowen, A. T. Brunger and B. R. Lentz, *Biophys. J.*, 2006, **90**, 1661–75.

23. F. Quemeneur, J. K. Sigurdsson, M. Renner, P. J. Atzberger, P. Bassereau and D. Lacoste, *Proc. Natl. Acad. Sci. U. S. A.*, 2014, **111**, 5083–7.

24. T. Pott, H. Bouvrais and P. Méléard, *Chem. Phys. Lipids*, 2008, **154**, 115–9.

25. S. Aimon, J. Manzi, D. Schmidt, J. A. Poveda Larrosa, P. Bassereau and G. E. S. Toombes, *PLoS One*, 2011, **6**, e25529.

26. P. Méléard and L. Bagatolli, in *Methods in Enzymology*, Volume 465., 2009, vol. 465, pp. 161–176.

27. H. Basit, S. G. Lopez and T. E. Keyes, *Methods*, 2014.

28. T. Tabarin, A. Martin, R. J. Forster and T. E. Keyes, *Soft Matter*, 2012, **8**, 8743.

29. S. Ramadurai, A. Holt, V. Krasnikov, G. van den Bogaart, J. A. Killian and B. Poolman, *J. Am. Chem. Soc.*, 2009, **131**, 12650–12656.

30. D. S. Banks and C. Fradin, *Biophys. J.*, 2005, **89**, 2960–71.

31. R. Machán and M. Hof, *Biochim. Biophys. Acta*, 2010, **1798**, 1377–91.

32. D. Scherfeld, N. Kahya and P. Schwille, *Biophys. J.*, 2003, **85**, 3758–68.

33. P. G. Saffman and M. Delbrück, *Proc. Natl. Acad. Sci. U. S. A.*, 1975, **72**, 3111–3.

34. Y. Gambin, R. Lopez-Esparza, M. Reffay, E. Sierecki, N. S. Gov, M. Genest, R. S. Hodges and W. Urbach, *Proc. Natl. Acad. Sci. U. S. A.*, 2006, **103**, 2098–102.

35. K. Weiß, A. Neef, Q. Van, S. Kramer, I. Gregor and J. Enderlein, *Biophys. J.*, 2013, **105**, 455–62.

36. M. Rocco, B. Spotorno and R. Hantgan, *Protein Sci.*, 1993, **141**, 1685–95.

37. N. Kahya, *Biochim. Biophys. Acta*, 2010, **1798**, 1392–8.

38. K. El Kirat and S. Morandat, *Biochim. Biophys. Acta*, 2007, **1768**, 2300–9.

39. K. Bacia, C. G. Schuette, N. Kahya, R. Jahn and P. Schwille, *J. Biol. Chem.*, 2004, **279**, 37951–5.

40. N. Kahya, D. a Brown and P. Schwille, *Biochemistry*, 2005, **44**, 7479–89.

41. P. Wonerow, A. Obergfell, J. I. Wilde, R. Bobe, N. Asazuma, T. Brdicka, A. Leo, B. Schraven, V. Horejsí, S. J. Shattil and S. P. Watson, *Biochem. J.*, 2002, **364**, 755–65.

42. A. P. Siegel, A. Kimble-Hill, S. Garg, R. Jordan and C. a Naumann, *Biophys. J.*, 2011, **101**, 1642–50.

43. B. Leitinger and N. Hogg, *J. Cell Sci.*, 2002, **115**, 963–72.

44. J. Juhasz, J. H. Davis and F. J. Sharom, *Biochem. J.*, 2010, **430**, 415–23.

45. B. Müller, H. G. Zerwes, K. Tangemann, J. Peter and J. Engel, *J. Biol. Chem.*, 1993, **268**, 6800–8.

46. O. Purrucker, S. Gonnenwein, A. Fortig, R. Jordan, M. Rusp, M. Barmann, L. Moroder, E. Sackmann and M. Tanaka, *Soft Matter*, 2007, **3**, 333.

47. D. Marquardt, J. A. Williams, J. J. Kinnun, N. Kučerka, J. Atkinson, S. R. Wassall, J. Katsaras and T. A. Harroun, *J. Am. Chem. Soc.*, 2014, **136**, 203–10.

48. E. Castellana and P. Cremer, *Surf. Sci. Rep.*, 2006, **61**, 429–444.

49. F. Heinemann, V. Betaneli, F. A. Thomas and P. Schwille, *Langmuir*, 2012, **28**, 13395–404.

50. A. J. Diaz, F. Albertorio, S. Daniel and P. S. Cremer, *Langmuir*, 2008, **24**, 6820–6.

51. D. Mainali and E. a Smith, *Eur. Biophys. J.*, 2013, **42**, 281–90.

52. D. S. Harburger and D. a. Calderwood, *J. Cell Sci.*, 2009, **122**, 1472–1472.

53. K. Gousset, W. F. Wolkers, N. M. Tsvetkova, A. E. Oliver, C. L. Field, N. J. Walker, J. H. Crowe and F. Tablin, *J. Cell. Physiol.*, 2002, **190**, 117–28.

54. S. Bodin, C. Soulet, H. Tronchère, P. Sié, C. Gachet, M. Plantavid and B. Payrastre, *J. Cell Sci.*, 2005, **118**, 759–69.

55. N. F. Hussain, A. P. Siegel, Y. Ge, R. Jordan and C. a Naumann, *Biophys. J.*, 2013, **104**, 2212–21.

56. J. L. McGregor and R. N. Poston, *J. Thromb. Haemost.*, 2003, **1**, 1142–3.